www.nature.com/aps

Acta Pharmacologica Sinica

ARTICLE

A novel compound AB38b attenuates oxidative stress and ECM protein accumulation in kidneys of diabetic mice through modulation of Keap1/Nrf2 signaling

Lei Du[1], Lei Wang[1], Bo Wang[1], Jin Wang[1], Meng Hao[1], Yi-bing Chen[1], Xi-zhi Li[1], Yuan Li[1], Yan-fei Jiang[1], Cheng-cheng Li[1], Hao Yang[1], Xiao-ke Gu[1], Xiao-xing Yin[1] and Qian Lu[1]

Extracellular matrix (ECM) deposition following reactive oxygen species (ROS) overproduction has a key role in diabetic nephropathy (DN), thus, antioxidant therapy is considered as a promising strategy for treating DN. Here, we investigated the therapeutic effects of AB38b, a novel synthetic α, β-unsaturated ketone compound, on the oxidative stress (OS) and ECM accumulation in type 2 diabetes mice, and tried to clarify the mechanisms underlying the effects in high glucose (HG, 30 mM)-treated mouse glomerular mesangial cells (GMCs). Type 2 diabetes model was established in mice with high-fat diet feeding combined with streptozocin intraperitoneal administration. The diabetic mice were then treated with AB38b (10, 20, 40 mg·kg^{-1}·d^{-1}, ig) or a positive control drug resveratrol (40 mg·kg^{-1}·d^{-1}, ig) for 8 weeks. We showed that administration of AB38b or resveratrol prevented the increases in malondialdehyde level, lactate dehydrogenase release, and laminin and type IV collagen deposition in the diabetic kidney. Simultaneously, AB38b or resveratrol markedly lowered the level of Keap1, accompanied by evident activation of Nrf2 signaling in the diabetic kidney. The underlying mechanisms of antioxidant effect of AB38b were explored in HG-treated mouse GMCs. AB38b (2.5−10 μM) or resveratrol (10 μM) significantly alleviated OS and ECM accumulation in HG-treated GMCs. Furthermore, AB38b or resveratrol treatment effectively activated Nrf2 signaling by inhibiting Keap1 expression without affecting the interaction between Keap1 and Nrf2. Besides, AB38b treatment effectively suppressed the ubiquitination of Nrf2. Taken together, this study demonstrates that AB38b ameliorates experimental DN through antioxidation and modulation of Keap1/Nrf2 signaling pathway.

Keywords: AB38b; resveratrol; antioxidant; diabetic nephropathy; oxidative stress; ECM; Nrf2; Keap1; glomerular mesangial cells

Acta Pharmacologica Sinica (2020) 41:358–372; https://doi.org/10.1038/s41401-019-0297-6

INTRODUCTION

Diabetic nephropathy (DN) is one of the most serious chronic complications of diabetes mellitus and affects ~30% of type 2 diabetes mellitus patients [1]. It is characterized by glomerular mesangial cell proliferation, mesangial hypertrophy, and an accumulation of the extracellular matrix (ECM) [2]. The pathogenesis of DN remains unclear, and hemodynamic changes, genetic susceptibility, hyperglycemia, dyslipidemia, and oxidative stress (OS) have been seen as promoting factors for DN [3]. Among these, OS and its related reactions serve important roles in the progression of DN [4]. On one hand, excessive OS activates multiple intracellular signaling pathways, such as the JNK and PKC pathways, and stimulates transcription factors, such as nuclear factor NF-κB and AP-1, thus resulting in the increased deposition of the ECM [5]. On the other hand, the high expression of products with related activity directly leads to reduced matrix degradation, which results in glomerulosclerosis and renal fibrosis [6].

The nuclear factor erythroid-derived 2-like 2 (Nrf2), as an important endogenous antioxidant transcription factor, protects cells from OS injury via interacting with antioxidant response element (ARE) [7–9] and then activates the transcription of downstream antioxidant enzymes, such as catalase (CAT), superoxide dismutase (SOD1 and SOD2), heme oxygenase-1 (HO-1), and NADPH quinone oxidoreductase (NQO-1) [10–12]. Kelch-like ECH-associated protein 1 (Keap1) has an important role in the Nrf2/ARE signaling pathway. In addition, Keap1-mediated Nrf2 ubiquitination and the phosphorylation of Nrf2 are the main regulators of Nrf2 [13]. Under basal conditions, Keap1, acting as an inhibitor, interacts with Nrf2 to form a complex to prevent the activation of Nrf2 by transcription [14]. However, in response to hyperglycemia-mediated OS, Nrf2 is released from Keap1 and is transported into the nucleus, resulting in the activation of downstream antioxidant genes [15–17]. Therefore, targeting Nrf2 can effectively ameliorate OS in DN [8, 18, 19].

According to basic mechanisms, several compounds with Nrf2 agonistic activity, such as sulforaphane and bardoxolone methyl, have been reported. Sulforaphane has been demonstrated to be beneficial for diabetic complications by promoting the nuclear accumulation of Nrf2 by changing the conformation of the cysteinyl residues of Keap1 [20–23]. Bardoxolone methyl, which is derived

[1]Jiangsu Key Laboratory of New Drug Research and Clinical Pharmacy, Xuzhou Medical University, Xuzhou 221004, China
Correspondence: Qian Lu (prairy@126.com)
These authors contributed equally: Lei Du, Lei Wang

Received: 8 April 2019 Accepted: 6 August 2019
Published online: 23 October 2019

from the natural product oleanolic acid, is an inducer of Nrf2 and was once seen as a promising new drug. However, a phase III clinical trial (BEACON) in patients with stage 4 CKD and type 2 diabetes was terminated because of its serious side effects, which are partly owing to the toxicity of the drug structure [17, 24].

Hence, therapies targeting oxygen biology, such as those that modulate Nrf2, have been considered promising therapeutic methods for DN [25]. However, identifying high-efficiency and low-toxicity Nrf2 agonists is of great importance.

AB38b is a novel synthetic α, β-unsaturated carbonyl compound with biphenyl diester (DDB) as its precursor. α, β-unsaturated carbonyl compounds, which act as Michael acceptors, have been found to covalently modify the cysteinyl residues of Keap1 to form covalent bonds and regulate related signaling pathways to have a role in disease prevention and treatment [26, 27]. Therefore, these α, β-unsaturated reactive ketones that function as chalcones are responsible for their biological activities. DDB is a synthetic intermediate of schisandrin C, a Chinese medicine herb used to treat hepatitis [28]. DDB has been reported to have various pharmacological effects, such as antiviral, antioxidant, immunomodulatory, and anticancer effects [29, 30]. Based on the evidence described above, a series of compounds containing these two structures, among which AB38b has shown excellent antioxidant activity and can activate Nrf2, have been designed and synthesized (Fig. 1e). However, whether AB38b can alleviate DN and the specific mechanism needs to be further studied and clarified.

In the present study, we focused on whether AB38b can alleviate OS and ECM accumulation in DN by modulating the Keap1/Nrf2 signaling pathway.

MATERIALS AND METHODS

Materials

AB38b (≥ 98% purity) was designed and synthesized by XiaoKe Gu (Xuzhou Medical University, Xuzhou, China) and was dissolved in dimethyl sulfoxide (DMSO) to generate a primary stock solution. The solution was stored at 4 °C and then diluted in medium before each in vitro experimental study. For in vivo studies, AB38b was dissolved in a 0.5% carboxy methyl cellulose (CMC) solution.

Animal model

Male C57BL/6 J mice weighing 20–25 g were obtained from the Laboratory Animal Centre of Xuzhou Medical University and the experiments were performed following the Guiding Principles for Care and Use of Laboratory Animals of Xuzhou Medical University. To generate the animal model, normal mice that were fed chow and provided water ad libitum were injected with 0.1 mol/L sodium citrate buffer, pH 4.5. The normal mice were randomly divided into two groups ($n = 9$/group): the control group (N) and the high-dose group (N + AB38bH). The mice were intragastrically treated with 40 mg/kg AB38b dissolved in a 0.5% CMC solution daily. In the DN group, the mice were fed a high glucose (HG)-fat diet for 8 weeks and then injected intraperitoneally with streptozocin (100 mg/kg in 0.1 mol/L sodium citrate buffer, pH 4.5). Mice with fasting blood glucose (FBG) levels above 13.9 mmol/L were considered diabetic. DN mice were randomly divided into five groups ($n = 9$/group): the model group (DN), the low-dose group (10 mg/kg AB38b), the medium-dose group (20 mg/kg AB38b), the high-dose group (40 mg/kg AB38b) and the positive control groups (40 mg/kg resveratrol). A 0.5% CMC solution was used for the control and model groups, whereas different concentrations of Res and AB38b were administered orally to the appropriate groups. After 8 weeks, the mice were placed in metabolic cages for urine collection, and blood samples were also collected. The animals were killed, and the kidneys were removed rapidly. The kidneys were stored at −80 °C for biochemical analysis.

Cell culture

The mouse glomerular mesangial SV40-MES-13 cell line (Fuxiang Biotechnology Company, Shanghai, China, ATCC number CRL-1927) was cultured in Dulbecco's modified Eagle's medium (DMEM) containing 100 units/mL penicillin, 100 mg/mL streptomycin, and 10% fetal bovine serum. Confluent cells were cultured in serum-free DMEM media for 24 h before the experiments. The cells were divided into the normal group (NG, 5.56 mM), the vehicle control group (DMSO, 0.05%, D5879, Sigma, St. Louis, MO, USA), the HG group (HG, 30 mM, G7021, Sigma), the HG + low-dose AB38b group (AB38bL + HG, 2.5 μM), the HG + medium-dose AB38b group (AB38bM + HG, 5 μM), the high glucose + high-dose AB38b group (AB38bH + HG, 10 μM), the high glucose + resveratrol (5010, Sigma) positive control group (Res + HG, 10 μM), the sulforaphane positive control group (S4441, Sigma) and the MG132 positive control group (S2619, Selleckchem, Houston, TX, USA).

Cytotoxicity assay

The mouse glomerular mesangial cells (GMCs) were cultured in 96-well microplates at a density of 5000 cells/well. Twenty-four hours after cultivation, the cells were serum starved and treated with H_2O_2 (400 μM, Beyotime Institute of Biotechnology, Nantong, China) and different concentrations of compounds. After exposure to the compounds for 24 h, a cytotoxicity assay was performed using a Cell Counting Kit-8 (Beyotime Institute of Biotechnology, Nantong, Jiangsu, China). The $OD_{450\ nm}$, the absorbance value at 450 nm, was read using a 96-well plate reader (BioTek, Winooski, VT, USA), and the $OD_{450\ nm}$ absorbance was proportional to the viability of the cells.

Measurement of renal function and biochemical parameters

Blood glucose was measured by test strips (The Johnson Laboratory, Las Vegas, NV, USA). Creatinine (Cr) and blood urea nitrogen (BUN) were determined using Cr and BUN assay kits. The levels of low-density lipoprotein cholesterol (LDL-C) and total cholesterol (T-CHO) were tested by assay kits (Jiancheng Bioengineering Institute, Nanjing, China).

Nuclear and cytoplasmic extraction

The cytoplasmic and nuclear fractions were separated with extraction reagents (NE-PER, Thermo Scientific, Waltham, MA, USA). In brief, ice-cold CER I was added to the cell pellet, and the tube was vortexed vigorously at the highest setting for 15 s to fully suspend the cell pellet. Then, the tube was incubated on ice for 10 min. Ice-cold CER II was added to the tube, and the tube was vortexed for 5 s and incubated on ice for 1 min. The tube was vortexed for 5 s, followed by centrifugation at 12 000 r/min for 5 min to precipitate the nuclei. The supernatant (cytoplasmic extract) was immediately transferred to a clean prechilled tube. This tube was placed on ice until use or storage.

Western blotting analysis

Homogenates of the glomeruli isolated from the renal cortex were prepared in lysis buffer (50 mM Tris-HCl, pH 7.6, 150 mM NaCl, 1 mmol/L ethylenediaminetetraacetic acid, 1% NP-40, 1 mM phenylmethylsulfonyl fluoride, 1 mM Na_3VO_4 and 20 mM NaF). The homogenates were incubated for 30 min at 4 °C and centrifuged at 12 000 × g for 15 min at 4 °C. SV40 cells were lysed in the lysis buffer described above and incubated at 4 °C for 30 min. Then, the lysates were centrifuged at 12 000 × g for 15 min at 4 °C. The protein concentrations were determined with a BCA Protein Assay Kit (Thermo Scientific) following the manufacturer's protocol. For immunoblotting, proteins (40–80 μg) were separated by 8% sodium dodecyl sulfate polyacrylamide gel electrophoresis and transferred to polyvinylidene difluoride membranes (Millipore, Bedford, MA, USA). Then, the membranes were blocked in phosphate-buffered saline (PBS) containing 5% bovine serum albumin (BSA) for 2 h at

room temperature and incubated with primary antibodies overnight at 4 °C. Nrf2, Keap1, laminin, and collagen IV antibodies were purchased from Abcam (Cambridge, Cambridgeshire, UK). NQO-1, HO-1, and β-actin antibodies were obtained from Bioworld Technology (St. Louis, MO, USA). The first antibodies were detected using alkaline phosphatase-conjugated immunoglobulin G (Bioworld Technology) at room temperature for 1 h. The membranes were developed colorimetrically by a BCIP/NBT alkaline phosphatase color development kit (Beyotime Institute of Biotechnology). The density of the bands was quantified by densitometric analysis using ImageJ software from the National Institutes of Health.

RNA isolation and real-time quantitative reverse transcription polymerase chain reaction (qPCR)

Total RNA was extracted with TRIZOL (Invitrogen, Carlsbad, CA, USA). The mRNA was reverse transcribed using an RT-Rever TraAce kit (Toyobo Co, Osaka, Japan). The cDNA was analyzed in duplicate reactions by qPCR using 0.2 mML gene-specific primers and 1 × LightCycler 480 SYBR green I Master (Roche Applied Science, Mannheim, Baden-Württemberg, Germany) in a total volume of 10 mL. qPCR was carried out in a LightCycler 480 (Roche Applied Science) using a thermal profile of 10 min at 95 °C followed by 50 cycles of 15 s at 95 °C, 30 s at 60 °C, a melting curve of 15 s at 95 °C, 60 s at 1 min, heating to 95 °C and cooling for 30 s at 4 °C. The results were analyzed using LightCycler 480 software (version 1.5, Roche Applied Science). The relative mRNA levels were analyzed using the ΔΔCt method. The primers (Sangon Biotech Corporation, Shanghai, China) used for gene amplification are listed in Table 1.

Malondialdehyde analysis

In the experiment, the content of malondialdehyde (MDA) in the cells was analyzed on an high-performance liquid chromatography (HPLC) apparatus (Agilent, Santa Clara, CA, USA) according to a previously described method [31]. The analytical column was an Agilent Zorbax SB-C18 (250 mm × 4.6 mm; Agilent Technologies). The chromatographic conditions were as follows: mobile phase of 0.2% acetic acid in acetonitrile = 62: 38, column temperature: room temperature, injection volume: of 50 μL, detection wavelength of 310 nm, and flow rate of 1 mL/min. The concentrations of MDA were calculated from a standard curve prepared from 1,1,3,3-tetraethoxypropane. The MDA content in the renal cortex was measured spectrophotometrically using assay kits (JieMei Bioengineering Institute, Shanghai, China) performed according to the manufacturer's instructions.

LDH, SOD, GSH, and CAT activity

The activities of lactate dehydrogenase (LDH), SOD, CAT, and the level of glutathione (GSH) in SV40 cells and the renal cortex were measured spectrophotometrically using assay kits (JieMei Bioengineering Institute) according to the manufacturer's instructions.

Table 1. Primer sequences for qRT-PCR

Gene	Primer sequence (5′–3′)
Keap1	Forward: GAAGAGGCGGCAGAAGAAG
	Reverse: GCTCCAGGGCTATGACAGAT
Nrf2	Forward: GACAAACATTCAAGCCGATTAGAGG
	Reverse: ACTTTATTCTTCCCTCTCCTGCGT
NQO-1	Forward: GGTATTACGATCCTCCCTCAACATC
	Reverse: GAGTACCTCCCATCCTCTCTTCTTC
HO-1	Forward: GGTGATGGCTTCCTTGTACC
	Reverse: AGTGAGGCCCATACCAGAAG
β-actin	Forward: AGAGGGAAATCGTGCGTGAC
	Reverse: CAATAGTGATGACCTGGCCGT

Immunoprecipitation (IP) analysis

GMCs were lysed with IP buffer on ice for 30 min and centrifuged at 12 000 × *g* for 15 min at 4 °C, and protein from the cell lysates was incubated with primary antibodies against Keap1 or Nrf2 at 4 °C for 12 h. Immune complexes were captured with TrueBlot IP beads (Santa Cruz Biotechnology, Santa Cruz, CA, USA) at 4 °C for 4 h. After they were rinsed three times with IP lysis buffer, the bound proteins were boiled for 5 min and then eluted before Western blot analysis was performed. The protein bands were resolved and blotted with an anti-Keap1, anti-Nrf2 or anti-ubiquitin antibody at 4 °C for 12 h.

Morphological analysis and IHC

Kidney samples were fixed in 4% paraformaldehyde and embedded in paraffin. Sections that were 4-μm thick were cut for morphometric analysis and IHC. The sections were prepared for periodic acid-Schiff (PAS) and Sirius red staining, as described previously [32]. For immunohistological studies, immunoreactivity was detected in cortical sections with a specific primary antibody and an ABC staining kit and visualized with a DAB detection kit (both kits were obtained from Vector Laboratories Inc., Burlingame, CA, USA). Primary antibodies against collagen IV (1:200) and laminin (1:200) were obtained from Abcam. The sections were examined using an Olympus BX43F microscope. Linear measurements were obtained using an image analysis system (Image-Pro Plus 4.0, Media Cybernetics, Silver Spring, MD, USA).

Cell immunofluorescence (IF)

Mesangial cells were seeded onto round glass dishes and then subjected to various treatments. After they were washed three times with cold PBS, the cells were fixed with cold methanol at − 20 °C for 15 min and then incubated in blocking buffer (1% BSA and 0.1% Triton X-100 in PBS, pH 7.4) for 30 min at room temperature. The cells were subsequently incubated with Nrf2 (1:200), Keap1 (1:100), collagen IV (1:200), and laminin (1:100) primary antibodies for 12 h at room temperature. Then, the cells were washed three times with PBS and incubated with a secondary antibody conjugated to DyLight 594 or DyLight 488 (Earthox, Millbrae, CA, USA) at 37 °C for 1 h in the dark. The cell nuclei were stained with DAPI (Beyotime Institute of Biotechnology) for 1 min. Coverslips were mounted onto the glass slides, and the cells were viewed with an Olympus BX43F fluorescence microscope (Tokyo, Japan).

Measurement of intracellular ROS

The fluorescent probe 2′,7′-dichlorofluorescin diacetate (DCFH-DA, Sigma) was applied to evaluate the intracellular ROS levels. Cells were grown in six-well plates, and after being treated with different concentrations of AB38b or Res, the cells were incubated with 10 μM DCFH-DA at 37 °C for 25 min. Then, the distribution of DCF fluorescence in 10 000 cells was measured by flow cytometry (Miltenyi Biotec, Bergisch Gladbach, Nordrhein-Westfalen, Germany) at an excitation wavelength of 488 and an emission wavelength of 525 nm.

Statistical analysis

The statistical analysis of the experimental data was performed using SPSS 16.0 software, and the results are presented as the mean ± SD (standard deviation). Statistical differences were determined using analysis of variance followed by Dunnett's test (Exp. versus Con.) using one trial analysis. A significant difference was defined as $P < 0.05$ compared with the control.

RESULTS

The protective effect of some new compounds on mesangial cells

The cytotoxicity of the new compounds in GMCs was investigated by the CCK8 assay. The results indicated that treatment with

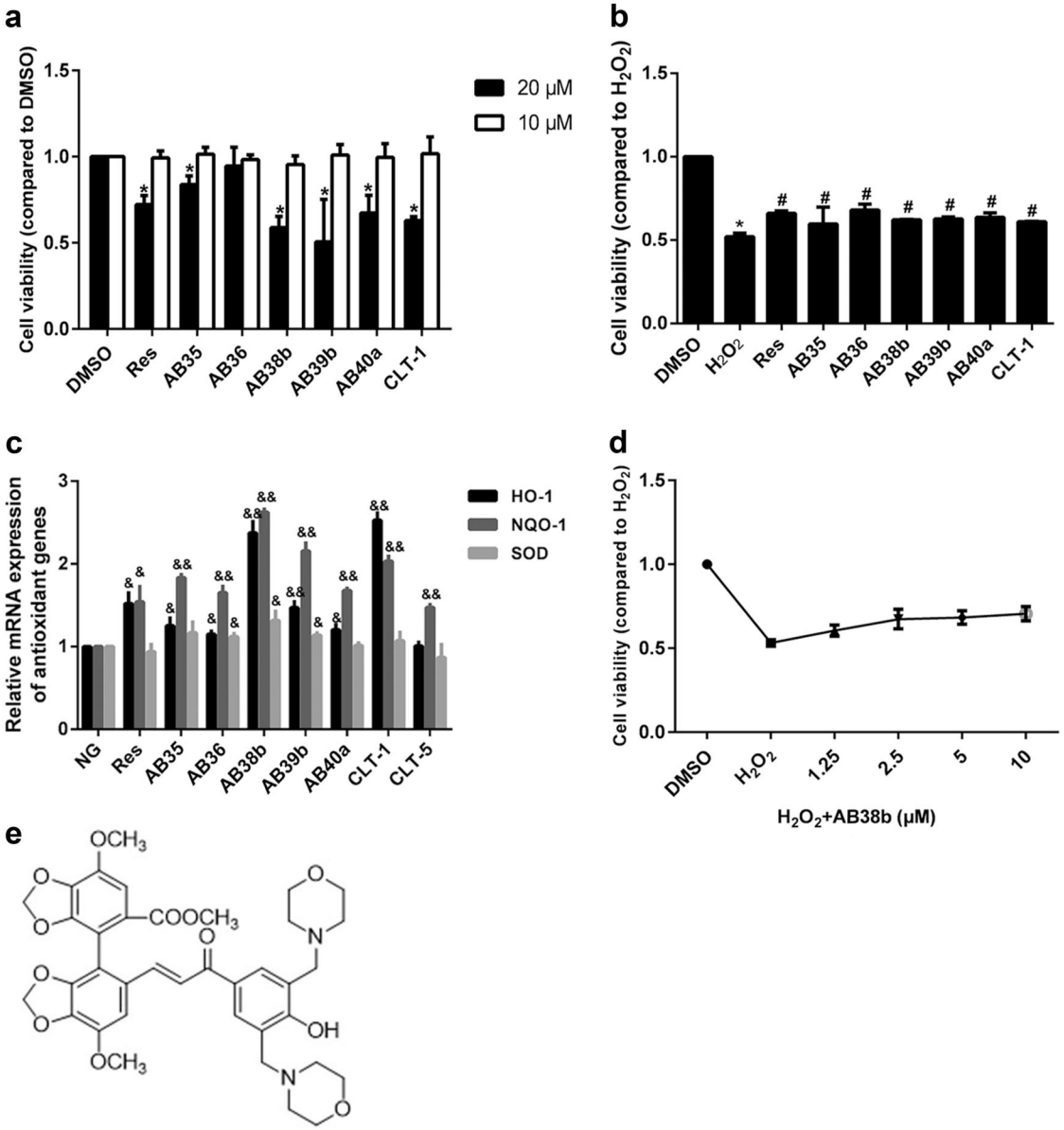

Fig. 1 Effects of some of the new compounds on cell viability. **a** Cells were treated with different compounds (20 μM, 10 μM) for 24 h, and cell viability was evaluated by the CCK8 assay. **b** The protective effect of the compounds on GMCs after H_2O_2-induced cell damage. **c** Compared with normal glucose (NG), the compounds (10 μM), and Res (10 μM) enhanced the transcription of the antioxidant genes NQO-1, HO-1, and SOD. **d** The concentration-dependent effect of AB38b on cell viability. **e** The chemical structure of AB38b. The data are expressed as the mean ± SD, $n = 3$. $^{*}P < 0.05$ vs. DMSO; $^{\#}P < 0.05$ vs. H_2O_2; $^{\&}P < 0.05$, $^{\&\&}P < 0.01$ vs. NG

10 μM of the compounds for 24 h did not produce any significant cytotoxic effects, whereas 20 μM significantly decreased cell viability (Fig. 1a). To further evaluate whether the new compounds can protect GMCs against oxidative damage, cell viability was measured. Treatment with 10 μM of the new compounds reduced the cell growth inhibition caused by H_2O_2 (Fig. 1b). Given the cytotoxicity of the dose of 20 μM, a dose of 10 μM of the compounds was used to investigate their effects on antioxidant genes. Compared with those of the normal group (NG), the mRNA levels of HO-1, NQO-1, and SOD were increased significantly (Fig. 1c) in the group treated with the compounds, among which AB38b (Fig. 1e) showed excellent antioxidant activity. Treatment with AB38b increased cell viability suppressed by H_2O_2 in a dose-dependent manner (Fig. 1d). Therefore, doses of 2.5, 5, and 10 μM AB38b were used in the subsequent experiments to examine its role against OS and its potential ability to protect against DN.

AB38b reversed the alterations in biochemical parameters in diabetic mice

The FBG levels, body weight, and kidney weight-to-body weight ratio of the experimental mice were examined. Compared with those of the normal control mice, the FBG levels and the kidney weight-to-body weight ratio of the diabetic mice were significantly increased (Table 2). AB38b treatment had no effect on the FBG levels or kidney index of the mice. However, AB38b markedly reduced serum urine nitrogen (BUN, Fig. 2a), serum creatinine (Cr, Fig. 2b), LDL-C (Fig. 2c), and T-CHO (Fig. 2d) levels in diabetic mice in a dose-dependent manner, and AB38b treatment had no effect on normal control mice, suggesting that AB38b improved renal function in diabetic mice.

AB38b reduced ECM deposition and morphological changes in diabetic kidneys

PAS staining showed that glycogen deposition was enhanced in diabetic mice compared with control mice; however, this enhancement was alleviated in diabetic mice treated with AB38b (Fig. 3a, f). Sirius red staining was used to evaluate the severity of renal fibrosis in diabetic mice. Compared with that in normal control mice, the distribution of Sirius red-positive areas was significantly increased in diabetic mice, indicating collagen accumulation in both the glomerular and renal interstitium. The administration of AB38b reduced collagen deposition to different degrees (Fig. 3b, g). EM revealed that extensive foot process fusion occurred in the kidneys of diabetic mice (Fig. 3c–2 vs. c–1). Moreover, laminin and collagen IV expression, as measured by IHC, was increased in untreated diabetic mice compared with control mice (Fig. 3d–2 vs. d–1, and e–2 vs. e–1), however, these changes were significantly reversed by AB38b in a dose-dependent manner, and AB38b treatment had no effect on normal mice (Fig. 3d, e, h, i). These data suggest that AB38b dramatically ameliorates the glomerular damage, foot process fusion, and ECM deposition noted in the kidneys of diabetic mice.

Table 2. Effects of AB38b on kidney function of diabetic rats

Groups ($n = 6$)	Fasting blood glucose (mmol/L)	Body weights (g)	Kidney index (g/kg)
N	7.22 ± 0.56	30.65 ± 0.85	10.70 ± 0.56
DN	23.28 ± 2.43**	23.73 ± 1.23**	15.28 ± 1.24**
DN + AB38bL	21.27 ± 1.66	24.38 ± 0.87	13.99 ± 0.48
DN + AB38bM	18.80 ± 2.74	25.57 ± 1.36	12.64 ± 0.44
DN + AB38bH	14.32 ± 3.13#	24.94 ± 1.78	12.45 ± 0.39#
DN + Res	15.23 ± 6.44	25.08 ± 1.49	13.35 ± 1.32
N + AB38bH	6.93 ± 0.54	29.91 ± 0.49	11.07 ± 0.71

N control group, *DN* the model group, *DN + AB38bL* low-dose group (AB38b of 10 mg/kg), *DN + AB38bM* medium-dose group (AB38b of 20 mg/kg), *DN + AB38bH* high-dose group (AB38b of 40 mg/kg), *DN + Res* positive control groups (resveratrol of 40 mg/kg), *N + AB38bH* control group + AB38b of 40 mg/kg

Data are expressed as the mean ± SD, $n = 6$. $^{**}P < 0.01$ vs. N; $^{\#}P < 0.05$ vs. DN

AB38b alleviated OS and concomitantly activated Nrf2 in diabetic mice

Compared with those in normal control mice, the levels of MDA and LDH were markedly increased in the kidney cortex of diabetic mice. In contrast, the GSH level and CAT and SOD activities were obviously decreased. Treatment with AB38b effectively reversed these changes (Fig. 4a–e). The protein and gene expression of Nrf2, NQO-1, and HO-1 in the kidney cortex were examined by western blot and qRT-PCR. Diabetic mice exhibited decreased protein levels of Nrf2, NQO-1, and HO-1 in renal cortex homogenates, whereas the protein levels of Keap1 were obviously

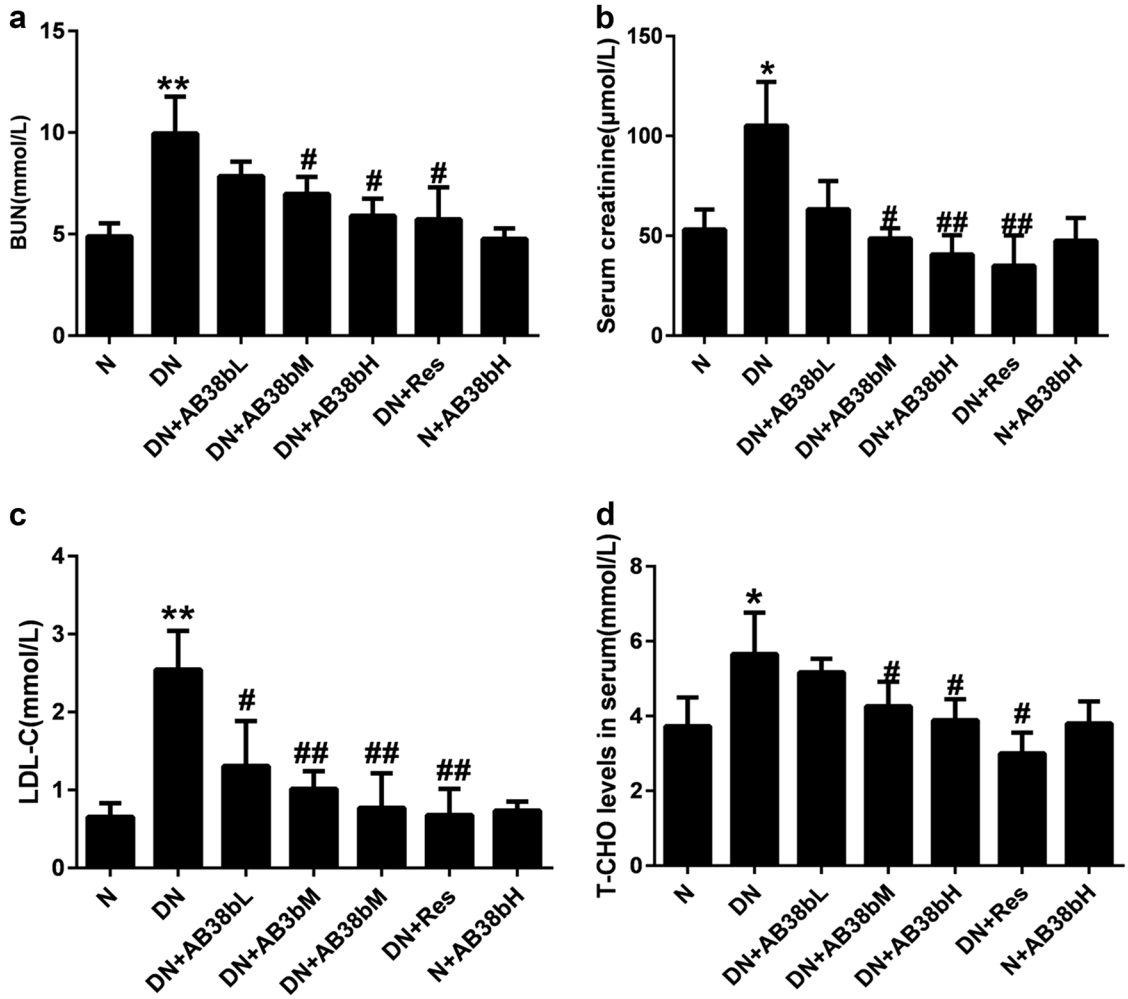

Fig. 2 Changes in physiological parameters in diabetic animals after AB38b treatment. **a** BUN, blood urea nitrogen. **b** Cr, serum creatinine. **c** LDL-C, low-density lipoprotein cholesterol. **d** T-CHO total cholesterol. The data are expressed as the mean ± SD, $n = 6$. $^{*}P < 0.05$, $^{**}P < 0.01$ vs. N; $^{\#}P < 0.05$, $^{\#\#}P < 0.01$ vs. DN

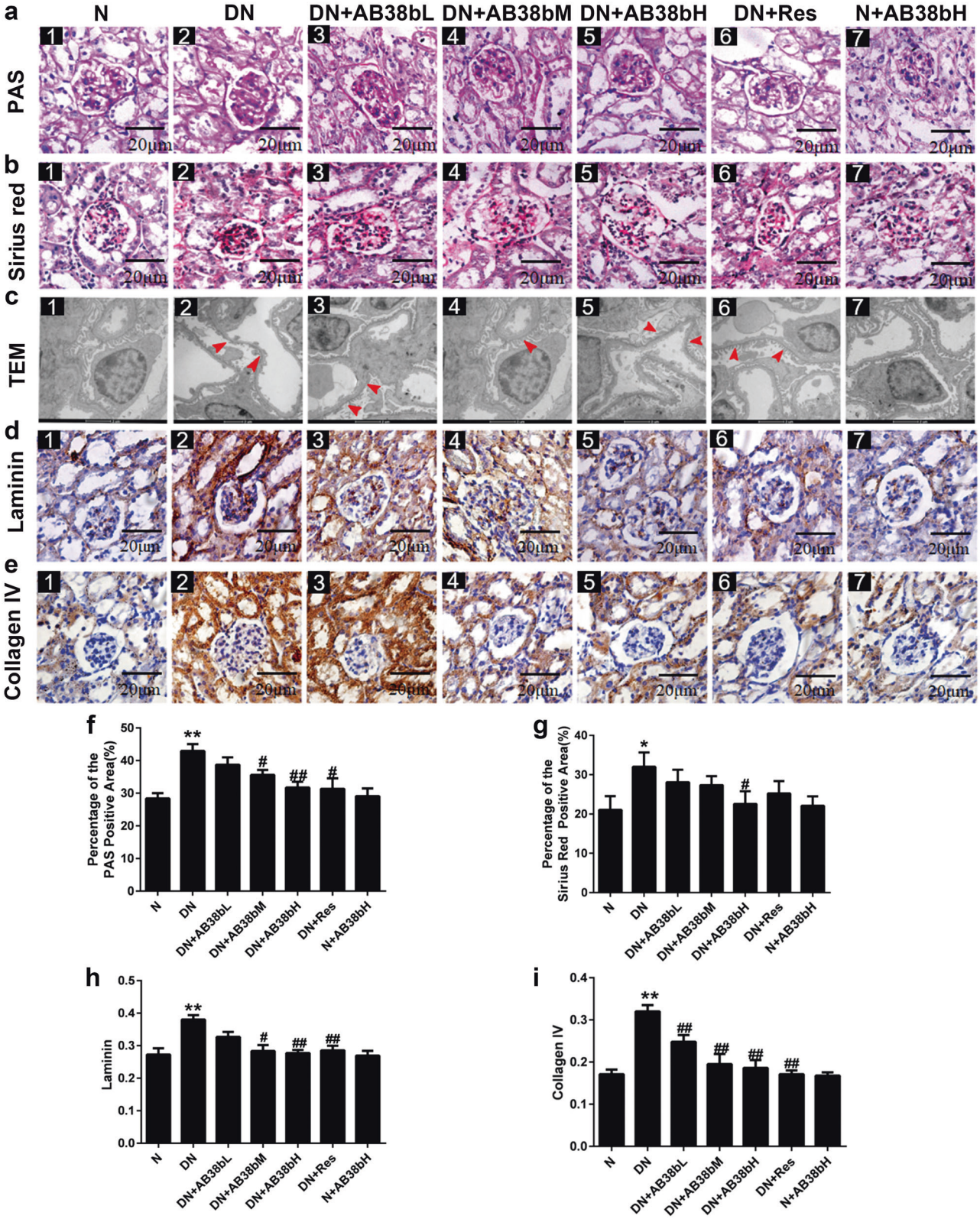

Fig. 3 Effects of AB38b on morphological changes and renal fibrosis in the glomeruli of diabetic animals. **a** PAS staining of the glomerulus. **b** Sirius red staining of the glomerulus. **c** TEM analysis. **d** Immunohistochemical analysis of laminin. **e** Immunohistochemical analysis of collagen IV. **f** Relative percentages of PAS staining. **g** Relative percentages of Sirius red staining. **h** The quantification of laminin expression. **i** The quantification of collagen IV expression. The data are expressed as the mean ± SD, $n = 6$. $^{*}P < 0.05$, $^{**}P < 0.01$ vs. N; $^{\#}P < 0.05$, $^{\#\#}P < 0.01$ vs. DN

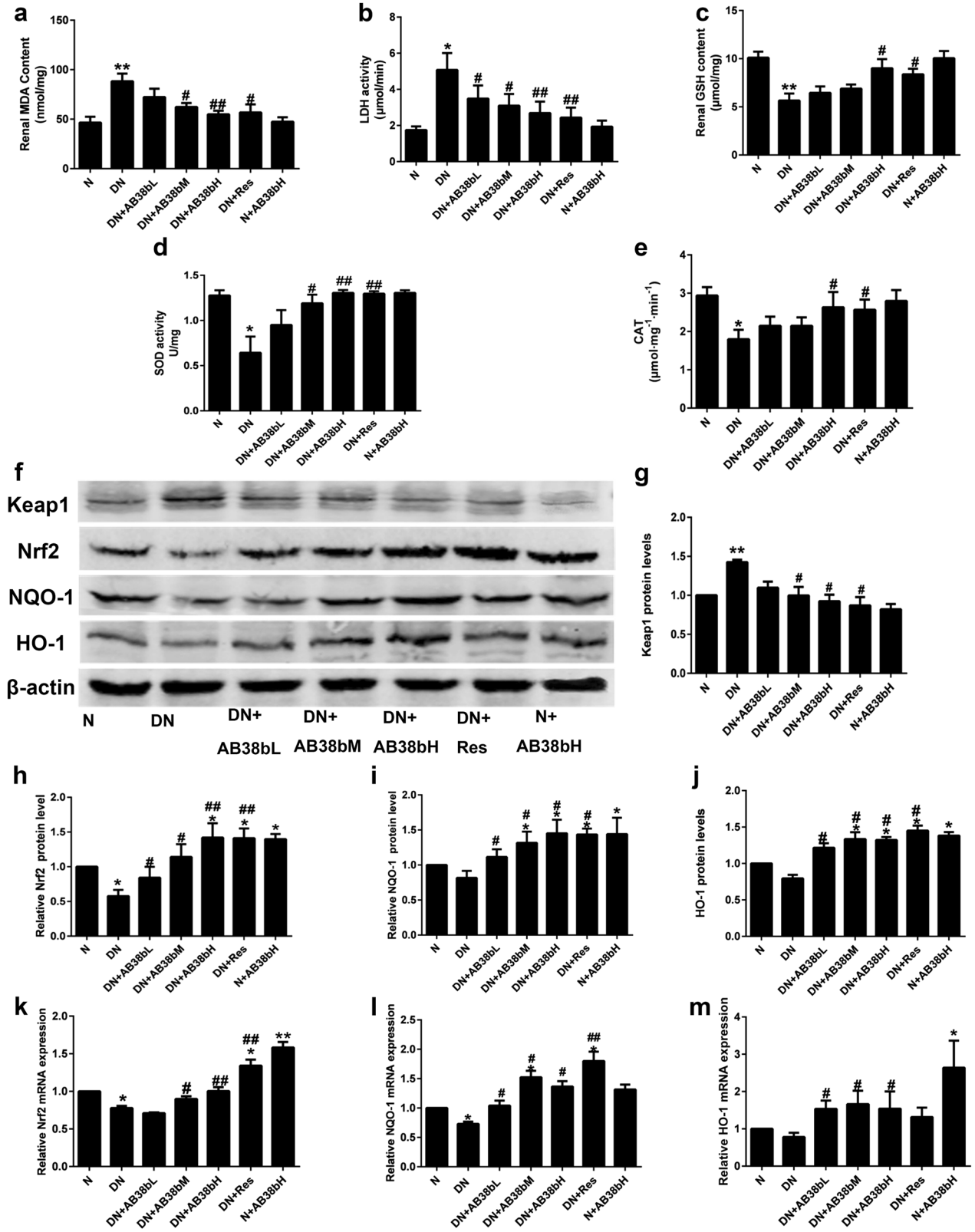

Fig. 4 AB38b reduced oxidative stress while activating Nrf2 in diabetic kidneys. **a** MDA levels. **b** LDH activity. **c** GSH levels. **d** SOD activity. **e** CAT levels. **f** Protein levels of Keap1, Nrf2, NQO-1, and HO-1. **g**–**j** The densitometric analysis of the Western blots. The Keap1 **g**, Nrf2 **h**, NQO-1 **i**, and HO-1 **j** signals were normalized to the β-actin signals for the same samples to determine the fold-change relative to the control, the expression level of which was set as 1. **k**–**m** The relative mRNA expression levels of Nrf2 **k**, NQO-1 **l**, and HO-1 **m** in diabetic kidneys. The data are expressed as the mean ± SD, $n = 6$. $^{*}P < 0.05$, $^{**}P < 0.01$ vs. N; $^{\#}P < 0.05$, $^{\#\#}P < 0.01$ vs. DN

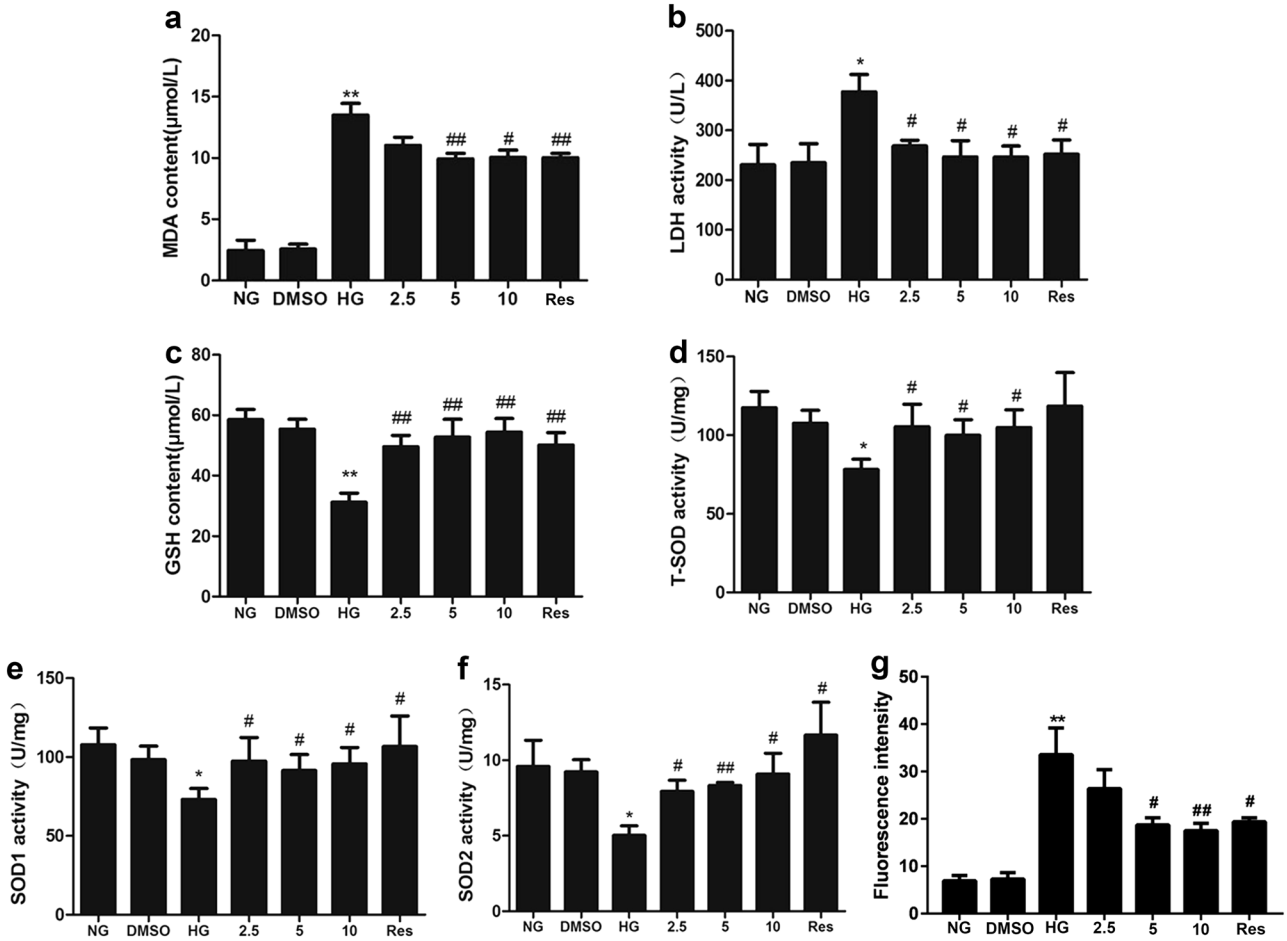

Fig. 5 AB38b alleviated HG-induced oxidative stress in mesangial cells. Mesangial cells were treated with various concentrations of AB38b (2.5 μM, 5 μM, and 10 μM) and Res (10 μM) with or without normal glucose (NG, 5.6 mM), high glucose (HG, 30 mM) or DMSO (0.05%) for 24 h. The MDA level, GSH level, LDH activity, T-SOD activity, SOD1 activity, SOD2 activity and the intracellular production of ROS in GMCs were detected to evaluate oxidative stress. **a** MDA levels. **b** LDH activity. **c** GSH levels. **d** T-SOD activity. **e** SOD1 activity. **f** SOD2 activity. **g** The intracellular production of ROS. The data are expressed as the mean ± SD, $n = 3$. $^{*}P < 0.05$, $^{**}P < 0.01$ vs. NG; $^{\#}P < 0.05$, $^{\#\#}P < 0.01$ vs. HG

increased. These changes were reversed by AB38b in a dose-dependent manner (Fig. 4f, j). The mRNA levels of Nrf2, NQO-1, and HO-1 confirmed these results (Fig. 4k–m).

AB38b alleviated OS in HG-induced mesangial cells

To further verify the protective effects of AB38b on OS, HPLC was used to measure the levels of MDA in mesangial cells. Our data showed that MDA was significantly increased in the HG groups. As expected, 5 μM and 10 μM AB38b remarkably decreased the increase in MDA (Fig. 5a). In addition, AB38b blocked the high levels of LDH induced by HG (Fig. 5b). GSH activity and SOD levels in the HG group were lower than those of the NG group, whereas treatment with different concentrations of AB38b significantly increased GSH activity and SOD levels (Fig. 5c–f). As shown in Fig. 5g, 5 μM and 10 μM AB38b significantly reduced the intracellular ROS in SV40 cells. These results indicate that AB38b can ameliorate OS induced by HG in mesangial cells.

AB38b inhibited HG-induced ECM accumulation while enhancing the expression of Nrf2 and its downstream gene in mesangial cells

IF analysis revealed that AB38b exerted an inhibitory effect on the increased laminin and collagen IV expression in the HG group (Fig. 6a, b), and the effects of AB38b were dose-dependent. These advantageous effects paralleled the AB38b-induced transcriptional activation of Nrf2. To cope with HG-induced OS, the protein and gene levels of Nrf2, NQO-1, and HO-1 increased in the HG group. However, these changes were small and did not have a major influence on redox status or ECM component synthesis in mesangial cells, whereas treatment with different concentrations of AB38b prominently activated the Nrf2 signaling pathway in HG-treated mesangial cells (Fig. 7a–g) and reversed the increased expression of laminin and collagen IV (Fig. 6a, b). IF analysis confirmed these results, and the nuclear import of Nrf2 was further increased after the administration of low, medium, and high doses of AB38b (Fig. 7h, Nrf2 panel). In addition, AB38b blocked the high levels of Keap1 induced by HG (Fig. 7h, Keap1 panel). These results imply that AB38b activates Nrf2 by inhibiting the expression of Keap1, ultimately ameliorating OS and ECM accumulation.

Nrf2 was involved in the inhibitory effect of AB38b on ECM accumulation and OS

To further confirm the involvement of Nrf2 in the function of AB38b, we detected changes in ECM proteins (collagen IV and laminin) and the activity of antioxidant enzymes, including CAT, GSH, and SOD, in stable Nrf2 knockdown SV40 cells, which were treated with HG and 10 μM AB38b. As shown in Fig. 8a–c, after treatment with 10 μM AB38b, the protein levels of collagen IV and laminin were significantly decreased in HG-induced si-veh SV40 cells, whereas they were increased in HG-induced si-Nrf2 cells. In contrast, the levels of the antioxidant enzymes CAT (Fig. 8d), GSH (Fig. 8e) and SOD (Fig. 8f) displayed the opposite trends. These results

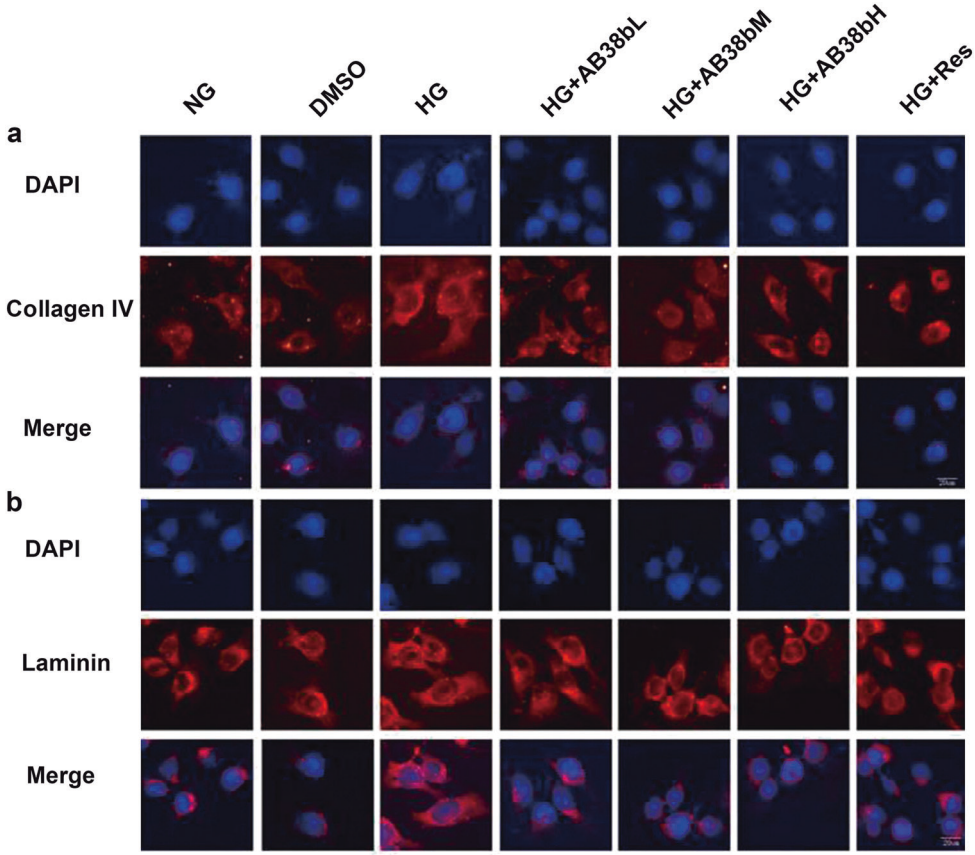

Fig. 6 Effects of AB38b on ECM accumulation in high glucose-induced mesangial cells. **a** IF analysis of collagen IV in SV40 cells exposed to HG conditions and treated with various concentrations of AB38b. **b** IF analysis of laminin in SV40 cells exposed to HG conditions and treated with various concentrations of AB38b

demonstrate that AB38b inhibits ECM accumulation and OS through Nrf2.

AB38b increased Nrf2, probably by inhibiting ubiquitination and degradation

To further explore the underlying mechanisms by which AB38b activates Nrf2, mesangial cells were divided into the vehicle control group (DMSO, 0.05%), the medium-dose AB38b group (5 μM), the positive control group (SFN, 2.5 μM), and the proteasome inhibitor group (MG132, 2.5 μM).

Compared with those in the DMSO group, the total Nrf2 protein and nucleoprotein levels in mesangial cells were significantly increased in the AB38b group (Fig. 9f, g), whereas the opposite results were observed for cytosolic Nrf2 expression in the AB38b group (Fig. 9h), indicating that AB38b can facilitate the nuclear import of Nrf2. The results were similar to those of the SFN group and MG132 group. In addition, total Nrf2 mRNA expression in the AB38b group showed no increase, whereas it slightly increased in the SFN group and MG132 group (Fig. 9b). In contrast, AB38b remarkably decreased the expression of Keap1. However, SFN and MG132 had no significant effect on Keap1 expression (Fig. 9c–e). The mRNA level of Keap1 confirmed these results (Fig. 9a). IP assays utilizing Nrf2 and Keap1 antibodies showed that the interactions between Nrf2 and Keap1 were significantly reduced in mesangial cells treated with SFN; however, there were no such changes in the AB38b group and MG132 group (Fig. 9i), implying that AB38b facilitates Nrf2 signaling by decreasing Keap1 expression without influencing the interactions between Nrf2 and Keap1.

Furthermore, AB38b, SFN, and MG132 significantly attenuated the activity of the 20 S proteasome (Fig. 9j), suggesting that AB38b has a key role in blocking the degradation of ubiquitin-conjugated proteins in mesangial cells by the 20 S complex. In addition, the ubiquitination of Nrf2 was measured after treatment with AB38b. The levels of ubiquitinated Nrf2 decreased when SV40 cells were treated with AB38b, however, these conjugated proteins significantly accumulated when the cells were incubated with the proteasome inhibitor MG132 (Fig. 9k). These results suggest that AB38b decreases Nrf2 degradation by inhibiting its ubiquitination.

DISCUSSION

The overproduction of reactive oxygen species (ROS) and the development of OS are common features of many kidney diseases, including DN [33, 34]. In addition, ROS are recognized as important mediators of several biological responses, including proliferation, ECM deposition, and apoptosis [5]. Increasing evidence has reported that therapies with antioxidant potential have beneficial effects on kidney diseases [35–37]. Therefore, the application of antioxidant agents against ROS stimulation in DN has attracted increasing attention. AB38b is a novel synthetic α, β-unsaturated carbonyl compound with DDB as its precursor. The results presented here indicate that AB38b increases the survival rate of mesangial cells and exerts significant protective effects against H_2O_2-induced damage. Considering the protective effects of AB38b in mesangial cells, we hypothesize that AB38b has a protective role in DN by inhibiting OS.

GMCs are the main type of cells that secrete ECM proteins and play a critical role in the progression of DN [38, 39]. Furthermore, it is well known that hyperglycemia is considered the main initiative factor in the progression of DN [40]. Exposure to a HG milieu

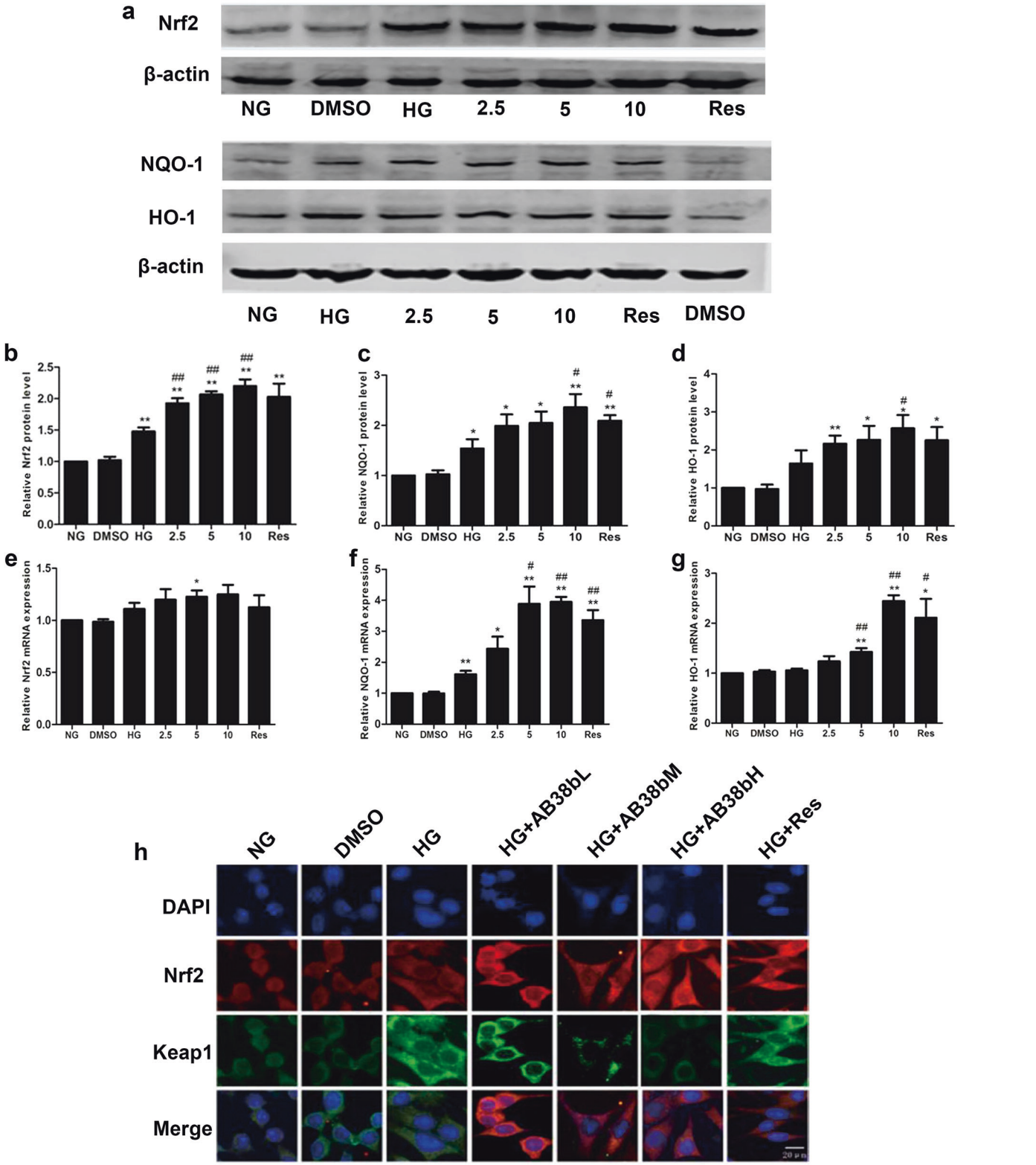

Fig. 7 Effects of AB38b on Nrf2 signaling in high glucose-induced mesangial cells. **a** Western blot analysis of Nrf2 (upper panel), NQO-1, and HO-1 (bottom panel) in the different groups of mesangial cells. **b**–**d** The densitometric analysis of the Western blots. The Nrf2 **b**, NQO-1 **c**, and HO-1 **d** signals were normalized to the β-actin signals for the same samples to determine the fold-change relative to the control, the expression level of which was set as 1. **e**–**g** The relative mRNA expression levels of Nrf2 **e**, NQO-1 **f**, and HO-1 **g** in the different groups of mesangial cells. **h** Confocal immunofluorescence images showing the colocalization of Nrf2 and Keap1 in SV40 cells exposed to HG conditions and treated with various concentrations of AB38b. The data are expressed as the mean ± SD, $n = 3$. $^{*}P < 0.05$, $^{**}P < 0.01$ vs. NG; $^{\#}P < 0.05$, $^{\#\#}P < 0.01$ vs. HG

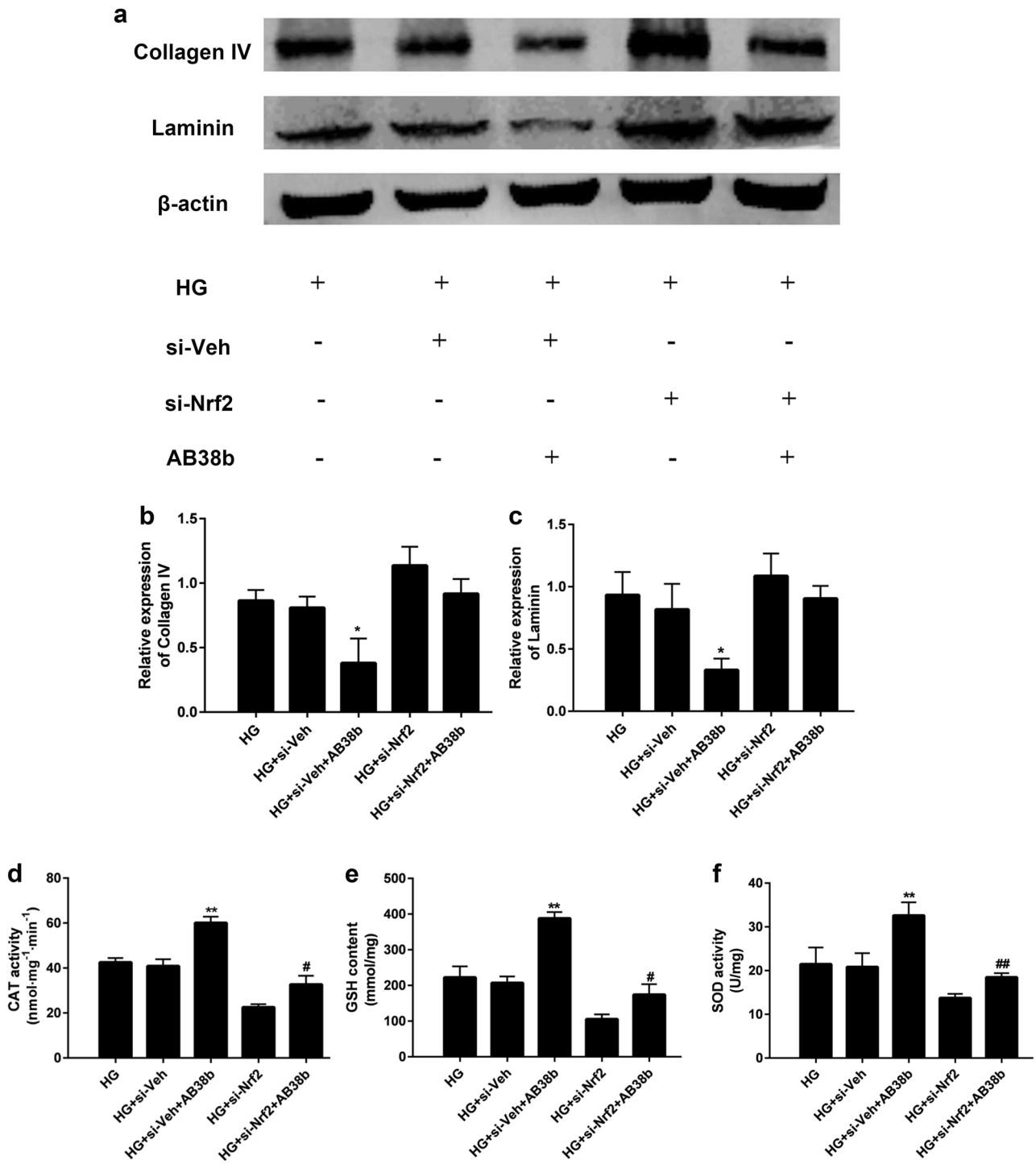

Fig. 8 Depletion of Nrf2 partly abrogated the inhibition of ECM components and increase of antioxidant enzymes by AB38b. **a** Western blot analysis of collagen IV and laminin in the different groups of mesangial cells. **b**–**c** The densitometric analysis of the Western blots. The collagen IV **b** and laminin **c** signals were normalized to the β-actin signals for the same samples to determine the fold-change relative to the control, the expression level of which was set as 1. **d**–**e** CAT activity **d**, GSH levels **e**, and SOD activity **f** in the different groups of mesangial cells. The data are expressed as the mean ± SD, $n = 3$. $^{*}P < 0.05$, $^{**}P < 0.01$ vs. HG + si-Veh; $^{\#}P < 0.05$, $^{\#\#}P < 0.01$ vs. HG + si-Nrf2

induces cell proliferation and ECM accumulation in GMCs, ultimately leading to DN [41, 42]. Thus, an in vitro HG model was established in mouse mesangial cells to evaluate the effects of AB38b on OS and ECM accumulation. Our results showed that HG stimulation obviously induced the expression of laminin and collagen IV in GMCs, the main components of the ECM. However, this elevation was abrogated by AB38b treatment in a dose-dependent manner. Similar to the results obtained in vitro, the in vivo study showed increased expression of laminin and collagen IV in the renal cortex of diabetic mice. This result is in line with that of another study in which the caffeamide derivative KS370G was administered to renal ischemia reperfusion injury (IRI) mice and renal tubular epithelial cells (NRK52E and HK-2) to verify its antifibrotic potential. KS370G ameliorated IRI through its ability

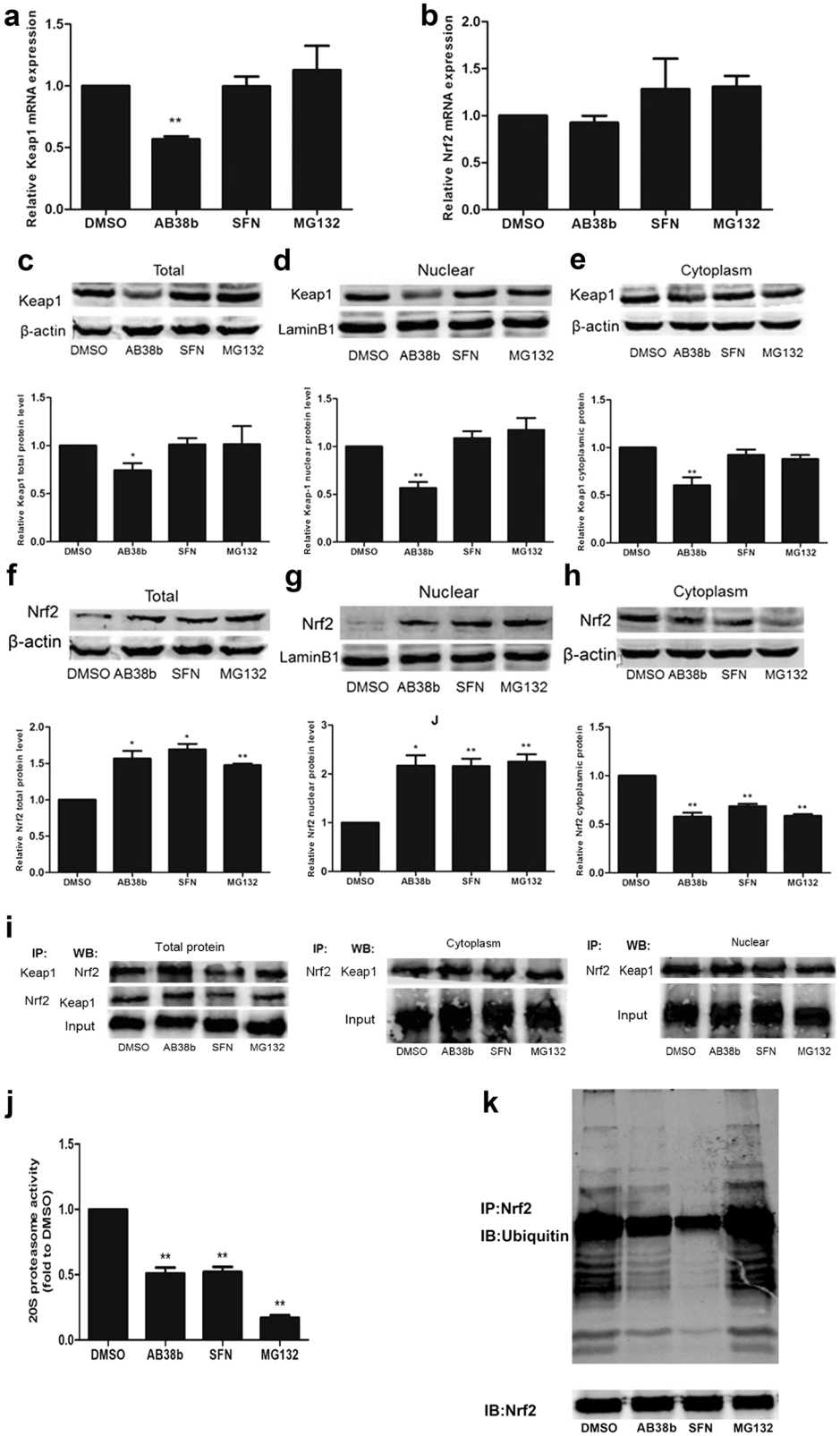

Fig. 9 AB38b exerted an antioxidant role via reducing cytoplasmic Keap1 and inhibiting the ubiquitination of Nrf2. Mesangial cells were treated with DMSO (0.05%), AB38b (5 μM), SFN (2.5 μM), and MG132 (2.5 μM) for 24 h. **a**–**b** The relative mRNA expression levels of Keap1 **a** and Nrf2 **b**. **c**–**h** The nuclear and cytosolic fractions were extracted from various groups as indicated and were used for immunoblot analysis of Keap1 **c**–**e** and Nrf2 **f**–**h**. **i** Co-IP and Western blot analysis showed interactions between Keap1 and Nrf2. **j** The activity of the 20 S proteasome. **k** The inhibitory effect of AB38b on ubiquitinated Nrf2 in SV40 cells. Total cell lysates were immunoprecipitated with an anti-Nrf2 antibody and then immunoblotted with an anti-ubiquitin antibody. The data are expressed as the mean ± SD, $n = 3$. $^{*}P < 0.05$, $^{**}P < 0.01$ vs. DMSO

to significantly reduce the IRI-induced accumulation of ECM proteins (collagen and fibronectin) in mice and in cells [43].

Furthermore, under persistent diabetic conditions, the renal function in these mice worsens significantly and the conventional parameters Cr, BUN, LDL-C, and T-CHO are elevated. However, treatment with AB38b improves these changes induced by diabetes. These results indicate that AB38b is an effective compound for protecting against and alleviating a decline in renal function and renal fibrosis. During periods of hyperglycemia, renal cells fail to attenuate the entrance of glucose into the cell, resulting in increased substrate levels for the mitochondrial electron transport chain, which leads to even more-reactive electron carriers and thus an enhanced production of ROS [44]. It is well known that antioxidant enzymes such as SOD, CAT, and GSH have synergistic roles in the clearance of oxygen free radicals [45]. In addition, MDA is considered the most-representative indicator of oxidative damage because it is a key product of lipid peroxidation [46]. In the current study, we found that GSH, T-SOD, and CAT were downregulated, whereas the MDA accumulated in HG-induced mesangial cells and diabetic mice. However, treatment with AB38b improved these changes, implying that AB38b can maintain the balance of OS under diabetic conditions and plays an important role in antioxidation. It is worth mentioning that the protective effect of a high dose of AB38b (10 μM) on antioxidant enzymes is similar to that of resveratrol. Several other studies are consistent with ours, showing that the anti-inflammatory conditions associated with diabetes are ameliorated by antioxidants and their synergistic potentials through the reduction of albumin and MDA [47–49].

Therefore, a better understanding of the molecular mechanisms underlying these effects is crucial. We previously observed that Nrf2 is a critical redox sensor and one of the master regulators of the antioxidant response [50, 51]. Nrf2 binds to regulatory AREs and activates the transcription of many antioxidant genes, such as HO-1 and NQO-1, which counteract ROS [52, 53]. To confirm the role of AB38b in the modulation of Nrf2 signaling in DN, real-time PCR, western blot, and IF staining were used to detect mRNA levels, protein expression, the distribution of Nrf2 expression and the levels of key antioxidant genes, including NQO-1 and HO-1. It is known that Nrf2 expression and function in cells (in vitro) are increased in response to OS, and several studies have indicated that HG can elevate Nrf2 expression and activation and the expression of its downstream gene in various cells [54]. Our findings are consistent with those of previous studies showing that HG stimulation obviously induces the nuclear protein levels of Nrf2 and upregulates NQO-1 and HO-1 levels. However, the increase in Nrf2 induced by HG is only a compensatory reaction of the body, and the protective effect of this reaction in cells and tissues cannot prevent the occurrence of DN. Nrf2 adaptively tries to remain functional to remove ROS and overcome diabetic damage in the early stage of diabetes. In the late stage of diabetes, however, antioxidant function is further impaired, leading to a decrease in Nrf2 expression [55, 56]. In agreement with these above studies, our in vivo study indicated that Nrf2 expression was decreased in the DN group compared with the control group. AB38b treatment greatly induced the expression of Nrf2 and its downstream targets NQO-1 and HO-1 in the DN group and control group. The results presented here indicate that AB38b activates Nrf2 signaling and exerts strong antioxidant activity, which may maintain long-term redox equilibrium in cells. Our data agree with another study in which antioxidant carnosol showed a protective antioxidant effect against OS through the activation of a pathway involving HO-1 in rat pheochromocytoma PC12 cells [57]. The oral administration of Protandim, a patented Nrf2 activator, in mdx mice (a mouse model of Duchenne muscular dystrophy) induced Nrf2 and HO-1 upregulation in SU5416/hypoxia-induced pulmonary hypertension and reduced OS in fatal heart disease and diaphragm fibrosis; it was also observed that osteopontin (a prominent biomarker of fibrosis) was reduced significantly. It was therefore concluded that the ability of Protandim to reduce osteopontin and OS may be attributed to its capacity to activate Nrf2/HO-1 signaling [58].

Several studies have indicated that Nrf2 activators such as resveratrol (Res), sulforaphane (SFN), and MG132 have protective effects against DN. Res can normalize the protein expression of Nrf2 and its downstream genes and has been used to prevent cancer, diabetes, and metabolic diseases, but its mechanism remains incompletely understood [59–61]. SFN interacts with Keap1 to disrupt Nrf2-Keap1 binding and allows for the nuclear accumulation of Nrf2 [62]. In addition, MG132 has a key role in blocking the degradation of ubiquitin-conjugated proteins by the 26 S complex [63]. Based on the above research status, we chose Res, SFN, and MG132 as positive controls to further explore the efficacy, mechanism and possible target of the AB38b-induced activation of Nrf2. In this study, we found that the protective effect of AB38b against DN and its excitatory effect on Nrf2 are consistent with those of Res. In addition, AB38b treatment greatly suppressed the expression of Keap1 and reduced the ubiquitination of Nrf2. These findings indicate that AB38b induces Nrf2 signaling by downregulating Keap1, suppressing the ubiquitination of Nrf2 and enhancing Nrf2 nuclear translocation.

In summary, our studies provide experimental evidence that AB38b inhibits OS and ECM expression induced by hyperglycemia in DN, at least in part by activating the Keap1/Nrf2 signaling pathway. Therefore, AB38b may be a potential agent for the treatment of DN.

ACKNOWLEDGEMENTS

The work was supported by the National Natural Science Foundation of China (No. 81473257), the Qing Lan project, the Natural Science Foundation of Jiangsu Province (No. BK20151155), the "333" Foundation of Jiangsu Province (No. BRA2015329), the Key Natural Science Foundation of Jiangsu Higher Education Institutions of China (No. 15KJA310005), the Jiangsu Overseas Research & Training Program for University Young & Middle-aged Teachers and Presidents, the Priority Academic Program Development of Jiangsu Higher Education Institutions (PAPD), and the Science and Technology Project of Xuzhou (No. KC18202).

AUTHOR CONTRIBUTIONS

XXY, QL, LD, LW, and MH contributed to the study design, manuscript preparation, and drafting of the manuscript. LW, LD, JW, MH, YBC, XZL, CCL, YL, and HY contributed to data collection, analysis, and revising the manuscript for important content. XKG and YFJ designed, synthesized, and analyzed the chemical compounds. All authors read and approved the final manuscript.

ADDITIONAL INFORMATION

Competing interests: The authors declare no competing interests.

REFERENCES

1. Du Y, Xu BJ, Deng X, Wu XW, Li YJ, Wang SR, et al. Predictive metabolic signatures for the occurrence and development of diabetic nephropathy and the intervention of *Ginkgo biloba* leaves extract based on gas or liquid chromatography with mass spectrometry. J Pharm Biomed Anal. 2019;166:30–9.
2. Liu YW, Hao YC, Chen YJ, Yin SY, Zhang MY, Kong L, et al. Protective effects of sarsasapogenin against early stage of diabetic nephropathy in rats. Phytother Res. 2018;32:1574–82.
3. Miranda-Diaz AG, Pazarin-Villasenor L, Yanowsky-Escatell FG, Andrade-Sierra J. Oxidative stress in diabetic nephropathy with early chronic kidney disease. J Diabetes Res. 2016;2016:7047238.
4. Han Q, Zhu H, Chen X, Liu Z. Non-genetic mechanisms of diabetic nephropathy. Front Med. 2017;11:319–32.
5. Sun Z, Ma Y, Chen F, Wang S, Chen B, Shi J. Artesunate ameliorates high glucose-induced rat glomerular mesangial cell injury by suppressing the TLR4/NF-kappaB/NLRP3 inflammasome pathway. Chem Biol Interact. 2018;293:11–9.
6. Ni WJ, Ding HH, Tang LQ. Berberine as a promising anti-diabetic nephropathy drug: an analysis of its effects and mechanisms. Eur J Pharmacol. 2015;760:103–12.

7. Chen YJ, Kong L, Tang ZZ, Zhang YM, Liu Y, Wang TY, et al. Hesperetin ameliorates diabetic nephropathy in rats by activating Nrf2/ARE/glyoxalase 1 pathway. Biomed Pharmacother. 2019;111:1166–75.
8. Zheng H, Whitman SA, Wu W, Wondrak GT, Wong PK, Fang D, et al. Therapeutic potential of Nrf2 activators in streptozotocin-induced diabetic nephropathy. Diabetes. 2011;60:3055–66.
9. Bryan HK, Olayanju A, Goldring CE, Park BK. The Nrf2 cell defence pathway: Keap1-dependent and -independent mechanisms of regulation. Biochem Pharmacol. 2013;85:705–17.
10. Kobayashi M, Yamamoto M. Molecular mechanisms activating the Nrf2-Keap1 pathway of antioxidant gene regulation. Antioxid Redox Signal. 2005;7:385–94.
11. Dreger H, Westphal K, Weller A, Baumann G, Stangl V, Meiners S, et al. Nrf2-dependent upregulation of antioxidative enzymes: a novel pathway for proteasome inhibitor-mediated cardioprotection. Cardiovasc Res. 2009;83:354–61.
12. Chowdhury SR, Sengupta S, Biswas S, Sen R, Sinha TK, Basak RK, et al. Low fucose containing bacterial polysaccharide facilitate mitochondria-dependent ROS-induced apoptosis of human lung epithelial carcinoma via controlled regulation of MAPKs-mediated Nrf2/Keap1 homeostasis signaling. Mol Carcinog. 2015;54:1636–55.
13. Li W, Jain MR, Chen C, Yue X, Hebbar V, Zhou R, et al. Nrf2 possesses a redox-insensitive nuclear export signal overlapping with the leucine zipper motif. J Biol Chem. 2005;280:28430–8.
14. Cuadrado A, Rojo AI, Wells G, Hayes JD, Cousin SP, Rumsey WL, et al. Therapeutic targeting of the NRF2 and KEAP1 partnership in chronic diseases. Nat Rev Drug Discov. 2019;18:295–317.
15. Jain AK, Bloom DA, Jaiswal AK. Nuclear import and export signals in control of Nrf2. J Biol Chem. 2017;292:2052.
16. Miyata T, de Strihou C. Diabetic nephropathy: a disorder of oxygen metabolism? Nat Rev Nephrol. 2010;6:83–95.
17. Liu YW, Liu XL, Kong L, Zhang MY, Chen YJ, Zhu X, et al. Neuroprotection of quercetin on central neurons against chronic high glucose through enhancement of Nrf2/ARE/glyoxalase-1 pathway mediated by phosphorylation regulation. Biomed Pharmacother. 2019;109:2145–54.
18. de Zeeuw D, Bekker P, Henkel E, Hasslacher C, Gouni-Berthold I, Mehling H, et al. The effect of CCR2 inhibitor CCX140-B on residual albuminuria in patients with type 2 diabetes and nephropathy: a randomised trial. Lancet Diabetes Endocrinol. 2015;3:687–96.
19. Aminzadeh MA, Nicholas SB, Norris KC, Vaziri ND. Role of impaired Nrf2 activation in the pathogenesis of oxidative stress and inflammation in chronic tubulointerstitial nephropathy. Nephrol Dial Transplant. 2013;28:2038–45.
20. Shang G, Tang X, Gao P, Guo F, Liu H, Zhao Z, et al. Sulforaphane attenuation of experimental diabetic nephropathy involves GSK-3 beta/Fyn/Nrf2 signaling pathway. J Nutr Biochem. 2015;26:596–606.
21. Townsend BE, Johnson RW. Sulforaphane induces Nrf2 target genes and attenuates inflammatory gene expression in microglia from brain of young adult and aged mice. Exp Gerontol. 2016;73:42–8.
22. Xu X, Luo P, Wang Y, Cui Y, Miao L. Nuclear factor (erythroid-derived 2)-like 2 (NFE2L2) is a novel therapeutic target for diabetic complications. J Int Med Res. 2013;41:13–9.
23. Keum YS. Regulation of the Keap1/Nrf2 system by chemopreventive sulforaphane: implications of posttranslational modifications. Ann N Y Acad Sci. 2011;1229:184–9.
24. Chin MP, Wrolstad D, Bakris GL, Chertow GM, de Zeeuw D, Goldsberry A, et al. Risk factors for heart failure in patients with type 2 diabetes mellitus and stage 4 chronic kidney disease treated with bardoxolone methyl. J Card Fail. 2014;20:953–8.
25. Miyata T, Suzuki N, van Ypersele, de Strihou C. Diabetic nephropathy: are there new and potentially promising therapies targeting oxygen biology? Kidney Int. 2013;84:693–702.
26. Jalonen U, Paukkeri EL, Moilanen E. Compounds that increase or mimic cyclic adenosine monophosphate enhance tristetraprolin degradation in lipopolysaccharide-treated murine j774 macrophages. J Pharmacol Exp Ther. 2008;326:514–22.
27. Sun H, Liu GT. Chemopreventive effect of dimethyl dicarboxylate biphenyl on malignant transformation of WB-F344 rat liver epithelial cells. Acta Pharmacol Sin. 2005;26:1339–44.
28. Abdel-Hameid NA. Protective role of dimethyl diphenyl bicarboxylate (DDB) against erythromycin induced hepatotoxicity in male rats. Toxicol In Vitro. 2007;21:618–25.
29. El-Beshbishy HA. The effect of dimethyl dimethoxy biphenyl dicarboxylate (DDB) against tamoxifen-induced liver injury in rats: DDB use is curative or protective. J Biochem Mol Biol. 2005;38:300–6.
30. He HJ, Wang GY, Gao Y, Ling WH, Yu ZW, Jin TR. Curcumin attenuates Nrf2 signaling defect, oxidative stress in muscle and glucose intolerance in high fat diet-fed mice. World J Diabetes. 2012;3:94–104.
31. Lu Q, Zhou Y, Hao M, Li C, Wang J, Shu F, et al. The mTOR promotes oxidative stress-induced apoptosis of mesangial cells in diabetic nephropathy. Mol Cell Endocrinol. 2018;473:31–43.
32. Lu Q, Ji XJ, Zhou YX, Yao XQ, Liu YQ, Zhang F, et al. Quercetin inhibits the mTORC1/p70S6K signaling-mediated renal tubular epithelial-mesenchymal transition and renal fibrosis in diabetic nephropathy. Pharmacol Res. 2015;99:237–47.
33. Lee HB, Yu MR, Yang Y, Jiang Z, Ha H. Reactive oxygen species-regulated signaling pathways in diabetic nephropathy. J Am Soc Nephrol. 2003;14:S241–5.
34. El Assar M, Angulo J, Rodriguez-Manas L. Oxidative stress and vascular inflammation in aging. Free Radic Biol Med. 2013;65:380–401.
35. Xu Y, Bai L, Chen X, Li Y, Qin Y, Meng X, et al. 6-Shogaol ameliorates diabetic nephropathy through anti-inflammatory, hyperlipidemic, anti-oxidative activity in *db/db* mice. Biomed Pharmacother. 2018;97:633–41.
36. Wang S, Zhao X, Yang S, Chen B, Shi J. Salidroside alleviates high glucose-induced oxidative stress and extracellular matrix accumulation in rat glomerular mesangial cells by the TXNIP-NLRP3 inflammasome pathway. Chem Biol Interact. 2017;278:48–53.
37. Kishore L, Kaur N, Singh R. Nephroprotective effect of *Paeonia emodi* via inhibition of advanced glycation end products and oxidative stress in streptozotocin-nicotinamide induced diabetic nephropathy. J Food Drug Anal. 2017;25:576–88.
38. Ke YQ, Liu C, Hao JB, Lu L, Lu NN, Wu ZK, et al. Morin inhibits cell proliferation and fibronectin accumulation in rat glomerular mesangial cells cultured under high glucose condition. Biomed Pharmacother. 2016;84:622–27.
39. Yang X, Wang Y, Gao G. High glucose induces rat mesangial cells proliferation and MCP-1 expression via ROS-mediated activation of NF-kappaB pathway, which is inhibited by eleutheroside E. J Recept Signal Transduct Res. 2016;36:152–7.
40. Brownlee M. The pathobiology of diabetic complications: a unifying mechanism. Diabetes. 2005;54:1615–25.
41. Madonna R, De Caterina R. Cellular and molecular mechanisms of vascular injury in diabetes–part I: pathways of vascular disease in diabetes. Vascul Pharmacol. 2011;54:68–74.
42. Kolset SO, Reinholt FP, Jenssen T. Diabetic nephropathy and extracellular matrix. J Histochem Cytochem. 2012;60:976–86.
43. Wang J, Fang H, Dong B, Wang D, Li Y, Chen X, et al. Effects of free anthraquinones extract from the Rhubarb on cell proliferation and accumulation of extracellular matrix in high glucose cultured-mesangial cells. Korean J Physiol Pharmacol. 2015;19:485–9.
44. Wagener FA, Dekker D, Berden JH, Scharstuhl A, van der Vlag J. The role of reactive oxygen species in apoptosis of the diabetic kidney. Apoptosis. 2009;14:1451–8.
45. Ozmen B, Ozmen D, Erkin E, Guner I, Habif S, Bayindir O. Lens superoxide dismutase and catalase activities in diabetic cataract. Clin Biochem. 2002;35:69–72.
46. Olofsson EM, Marklund SL, Karlsson K, Brannstrom T, Behndig A. In vitro glucose-induced cataract in copper-zinc superoxide dismutase null mice. Exp Eye Res. 2005;81:639–46.
47. Du X, Edelstein D, Brownlee M. Oral benfotiamine plus alpha-lipoic acid normalises complication-causing pathways in type 1 diabetes. Diabetologia. 2008;51:1930–2.
48. Rojas-Rivera J, Ortiz A, Egido J. Antioxidants in kidney diseases: the impact of bardoxolone methyl. Int J Nephrol. 2012;2012:321714.
49. Fallahzadeh MK, Dormanesh B, Sagheb MM, Roozbeh J, Vessal G, Pakfetrat M, et al. Effect of addition of silymarin to renin-angiotensin system inhibitors on proteinuria in type 2 diabetic patients with overt nephropathy: a randomized, double-blind, placebo-controlled trial. Am J Kidney Dis. 2012;60:896–903.
50. Ungvari Z, Bailey-Downs L, Gautam T, Jimenez R, Losonczy G, Zhang C, et al. Adaptive induction of NF-E2-related factor-2-driven antioxidant genes in endothelial cells in response to hyperglycemia. Am J Physiol Heart Circ Physiol. 2011;300:H1133–40.
51. Negi G, Kumar A, Joshi RP, Sharma SS. Oxidative stress and Nrf2 in the pathophysiology of diabetic neuropathy: old perspective with a new angle. Biochem Biophys Res Commun. 2011;408:1–5.
52. Li B, Liu S, Miao L, Cai L. Prevention of diabetic complications by activation of Nrf2: diabetic cardiomyopathy and nephropathy. Exp Diabetes Res. 2012;2012:216512.
53. Tan Y, Ichikawa T, Li J, Si Q, Yang H, Chen X, et al. Diabetic downregulation of Nrf2 activity via ERK contributes to oxidative stress-induced insulin resistance in cardiac cells in vitro and in vivo. Diabetes. 2011;60:625–33.
54. Foresti R, Bucolo C, Platania CM, Drago F, Dubois-Rande JL, Motterlini R. Nrf2 activators modulate oxidative stress responses and bioenergetic profiles of

human retinal epithelial cells cultured in normal or high glucose conditions. Pharmacol Res. 2015;99:296–307.
55. Jiang T, Huang Z, Lin Y, Zhang Z, Fang D, Zhang DD. The protective role of Nrf2 in streptozotocin-induced diabetic nephropathy. Diabetes. 2010;59:850–60.
56. He X, Kan H, Cai L, Ma Q. Nrf2 is critical in defense against high glucose-induced oxidative damage in cardiomyocytes. J Mol Cell Cardiol. 2009;46:47–58.
57. Martin D, Rojo AI, Salinas M, Diaz R, Gallardo G, Alam J, et al. Regulation of heme oxygenase-1 expression through the phosphatidylinositol 3-kinase/Akt pathway and the Nrf2 transcription factor in response to the antioxidant phytochemical carnosol. J Biol Chem. 2004;279:8919–29.
58. Hybertson BM, Gao B, Bose SK, McCord JM. Oxidative stress in health and disease: the therapeutic potential of Nrf2 activation. Mol Asp Med. 2011;32:234–46.
59. Zhang L, Pang S, Deng B, Qian L, Chen J, Zou J, et al. High glucose induces renal mesangial cell proliferation and fibronectin expression through JNK/NF-kappaB/NADPH oxidase/ROS pathway, which is inhibited by resveratrol. Int J Biochem Cell Biol. 2012;44:629–38.
60. Zhou X, Zhao Y, Wang J, Wang X, Chen C, Yin D, et al. Resveratrol represses estrogen-induced mammary carcinogenesis through NRF2-UGT1A8-estrogen metabolic axis activation. Biochem Pharmacol. 2018;155:252–63.
61. Palsamy P, Subramanian S. Resveratrol protects diabetic kidney by attenuating hyperglycemia-mediated oxidative stress and renal inflammatory cytokines via Nrf2-Keap1 signaling. Biochim Biophys Acta. 2011;1812:719–31.
62. Negi G, Kumar A, Sharma S. SNrf2 and NF-kappaB modulation by sulforaphane counteracts multiple manifestations of diabetic neuropathy in rats and high glucose-induced changes. Curr Neurovasc Res. 2011;8:294–304.
63. Luo ZF, Qi W, Feng B, Mu J, Zeng W, Guo YH, et al. Prevention of diabetic nephropathy in rats through enhanced renal antioxidative capacity by inhibition of the proteasome. Life Sci. 2011;88:512–20.